

Time-resolved fluorescence studies of flavodoxin. Fluorescence decay and fluorescence anisotropy decay of tryptophan in *Desulfovibrio* flavodoxins

H. R. M. Leenders, J. Vervoort, A. van Hoek, and A. J. W. G. Visser

Department of Biochemistry, Agricultural University, Dreijenlaan 3, 6703 HA Wageningen, The Netherlands

Received September 2, 1989/Accepted in revised form October 16, 1989

Abstract. The time-resolved fluorescence characteristics of tryptophan in flavodoxin isolated from the sulfate-reducing bacteria *Desulfovibrio vulgaris* and *Desulfovibrio gigas* have been examined. By comparing the results of protein preparations of normal and FMN-depleted flavodoxin, radiationless energy transfer from tryptophan to FMN has been demonstrated. Since the crystal structure of the *D. vulgaris* flavodoxin is known, transfer rate constants from the two excited states 1L_a and 1L_b can be calculated for both tryptophan residues (Trp 60 and Trp 140). Residue Trp 60, which is very close to the flavin, transfers energy very rapidly to FMN, whereas the rate of energy transfer from the remote Trp 140 to FMN is much smaller. Both tryptophan residues have the indole rings oriented in such a way that transfer will preferentially take place from the 1L_a excited state. The fluorescence decay of all protein preparations turned out to be complex, the parameter values being dependent on the emission wavelength. Several decay curves were analyzed globally using a model in which tryptophan is involved in some nanosecond relaxation process. A relaxation time of about 2 ns was found for both *D. gigas* apo- and holo-flavodoxin. The fluorescence anisotropy decay of both *Desulfovibrio* FMN-depleted flavodoxins is exponential, whereas that of the two holoproteins is clearly non-exponential. The anisotropy decay was analyzed using the same model as that applied for fluorescence decay. The tryptophan residues turned out to be immobilized in the protein. A time constant of a few nanoseconds results from energy transfer from tryptophan to flavin, at least for *D. gigas* flavodoxin. The single tryptophan residue in *D. gigas* flavodoxin occupies a position in the polypeptide chain remote from the flavin prosthetic group. Because of the close resemblance of steady-state and time-resolved fluorescence properties of tryptophan in both flavodoxins, the center to center distance between tryptophan and FMN in *D. gigas* flavodoxin is probably very similar to the distance between Trp 140 and FMN in *D. vulgaris* flavodoxin (i.e. 20 Å).

Key words: Flavodoxin – *Desulfovibrio* – Flavin – Tryptophan – Time-resolved fluorescence – Fluorescence depolarization – Rotational correlation time

Introduction

Time-resolved fluorescence spectroscopy has gained considerable attention because precise information about structure and dynamics of various biopolymers can be obtained (for general references see Rigler and Ehrenberg 1973, 1976; Cundall and Dale 1983; Lakowicz 1983; Beechem and Brand 1985). Particularly, protein fluorescence decay measurements have been widely used for probing tryptophan microenvironment and dynamics (Munro et al. 1979; Longworth 1983; Beechem and Brand 1985; Brand et al. 1985). Flavodoxins are low-potential electron-carrying proteins (molecular weight 15–25 kDa), which contain, as well as tryptophan, another chromophoric molecule, namely the non-covalently bound prosthetic group flavin mononucleotide (FMN) (for reviews on flavodoxins see Mayhew and Ludwig 1975; Simondson and Tollin 1980; Tollin and Edmondson 1980). The chemical and physical properties of flavodoxins, isolated from various organisms, have been extensively investigated with several spectroscopic techniques (Edmondson and Tollin 1971; D'Anna and Tollin 1972; Ryan and Tollin 1973; Eaton et al. 1975; Visser et al. 1977, 1980, 1983 a, 1987; Irwin et al. 1980; Vervoort et al. 1985, 1986). The crystal structures of a few flavodoxins in different redox states have been reported at high resolution (Watenpaugh et al. 1973; Burnett et al. 1974; Smith et al. 1983).

In this paper the results of time-resolved fluorescence of tryptophan residues determined in two flavodoxins are reported. The flavodoxins were isolated from the sulfate-reducing bacteria *Desulfovibrio vulgaris* and *Desulfovibrio gigas*. The 3-dimensional structure of *D. vulgaris* flavodoxin is known (Watenpaugh et al. 1973). This flavodoxin contains two tryptophan residues, one of which is adjacent to FMN and the other remote from

FMN. *D. gigas* flavodoxin has a single tryptophan residue (Fox and Heumann 1982). Although its exact location is not known, it is believed to be positioned remote from FMN. Both apo- and holo-flavodoxins were examined in order to monitor radiationless energy transfer from tryptophan to flavin. For *D. vulgaris* flavodoxin the results can be compared with theoretical transfer rates derived from the X-ray distances and orientations.

Time-resolved fluorescence spectra of the tryptophans in apo- and holoproteins were measured in order to investigate rapid relaxation processes in these proteins. The results are discussed with reference to the peculiar photophysics of tryptophan (Andrews and Forster 1974; Szabo and Rayner 1980; Chang et al. 1983; Petrich et al. 1983; Cross et al. 1983; Ichiye and Karplus 1983; Creed 1984). Polarized fluorescence decay measurements were used to investigate the rotational motion of the tryptophans in both flavodoxins.

A preliminary account of the results has been presented earlier (Visser and Van Hoek 1988).

Experimental procedures

Isolation and purification of flavodoxins

Desulfovibrio flavodoxins, purified as described earlier (LeGall and Hatchikian 1967; LeGall and Forget 1978), were a gift of Prof. J. LeGall (University of Georgia). They were distributed into vials and kept as stock solutions at -20°C . Prior to experiments a vial was thawed and gel-filtrated over Sephadex G25 with either 0.1 M Tris-HCl buffer pH 7.5 or 0.05 M potassium phosphate pH 7.0 (for temperature dependent measurements) to concentrations in the 1–10 μM region. Published extinction coefficients (Dubourdieu and LeGall 1970) were used to determine the concentrations.

Preparation of apoprotein

The apoproteins were prepared by the trichloroacetic acid precipitation method followed by dissolution in neutral buffer (Wassink and Mayhew 1975).

Steady-state fluorescence

Fluorescence spectra were measured on an Aminco-SPF 500 spectrofluorimeter with excitation wavelength at 295 nm and band widths of 4 nm both in excitation and emission. The absorbance at 295 nm was adjusted to 0.06. Both emission and excitation spectra were corrected. Fluorescence quenching experiments with KI were performed as described by Lehrer (1971). N-acetyl-L-tryptophan amide (NATA) served as a reference compound in both spectral and quenching experiments. In the quenching experiments integrated spectra were compared to the integrated spectrum of NATA taken under similar conditions.

Time-resolved fluorescence

Fluorescence decay measurements using a mode-locked argon-ion laser/synchronously-pumped dye laser system as the source of excitation, inherent data collection and subsequent data analysis have been described in detail elsewhere (Van Hoek et al. 1983, 1987; Van Hoek and Visser 1985; Visser et al. 1985; Vos et al. 1987). Tryptophan was selectively excited at 300 nm. Time- and wavelength-resolved fluorescence emission spectroscopy was performed at 20°C with a double monochromator (band width 6 nm) having a polarizer set at the magic angle in front of the entrance slit. Fluorescence decays were measured as a function of emission wavelength every 10 nm between 320 and 400 nm. Three-dimensional presentation of the results was as described by Easter et al. (1976). The wavelength- and time-resolved fluorescence intensity $I(\lambda, t)$ is given by:

$$I(\lambda, t) = h(\lambda) \cdot s(\lambda, t) \quad (1)$$

where

$$h(\lambda) = \frac{F(\lambda)}{\int_0^{\infty} s(\lambda, t) dt} \quad (2)$$

with the corrected steady-state fluorescence $F(\lambda)$ and the decay function $s(\lambda, t)$ which is taken to a first approximation as a triple-exponential function with amplitudes α_i and lifetimes τ_i :

$$s(\lambda, t) = \sum_i \alpha_i \exp[-t/\tau_i] \quad (3)$$

For fluorescence decay and anisotropy decay at a single wavelength a Schott 339 nm line filter (half band width 5 nm) was used.

Global analysis of fluorescence decay curves of apo- and holo-flavodoxins was performed using the procedure previously outlined by Knutson et al. (1983) and Beechem et al. (1985 a, b).

Energy transfer

Energy transfer is assumed to occur via the Förster mechanism of very weak dipole-dipole coupling (Förster 1965). The rate of transfer between tryptophan (donor) and flavin (acceptor) is given by:

$$k_{\text{DA}} = (8.79 * 10^{23}) \tau_r^{-1} R^{-6} \kappa^2 J n^{-4} \quad (4)$$

In this equation, τ_r is the radiative lifetime of tryptophan fluorescence taken as 20 ns (Hochstrasser and Negus 1984), n is the refractive index of the medium between donor and acceptor taken as 1.4 (Eisinger et al. 1969), and J is the spectral overlap integral given by:

$$J = \int_0^{\infty} \frac{F(\nu) \varepsilon(\nu)}{\nu^4} d\nu \quad (5)$$

where $F(\nu)$ is the normalized fluorescence spectrum of tryptophan on a wavenumber scale, $\varepsilon(\nu)$ is the molar decadic extinction coefficient of the flavin acceptor. From

spectral data we determined the overlap integrals for the two flavodoxins as $J(D. gigas) = 0.91 * 10^{-14} \text{ cm}^3/\text{M}$ and $J(D. vulgaris) = 0.77 * 10^{-14} \text{ cm}^3/\text{M}$. The geometric parameters are the distance R between the centers of donor and acceptor, given in Å in (4), and the so-called orientation factor κ^2 given by:

$$\kappa^2 = [\sin \theta_d \cdot \sin \theta_a \cdot \cos \delta - 2(\cos \theta_d \cdot \cos \theta_a)]^2 \quad (6)$$

where δ is the dihedral angle between the transition moments of donor and acceptor and θ_d and θ_a are the polar angles made by the donor and acceptor transition moments, respectively, with the separation vector.

Geometry of chromophores in *D. vulgaris* flavodoxin

Center to center distances and the polar and dihedral angles between the relevant tryptophan and FMN transition moments in *D. vulgaris* flavodoxin were calculated using the CHEM-X package, developed and distributed by Chemical Design Ltd., Oxford, England. The location of the transition moments in tryptophan and flavin was taken from the work of Yamamoto and Tanaka (1972) and of Johansson et al. (1979), respectively.

Results and discussion

The outline of this section is as follows. We first present some results of steady-state fluorescence spectroscopy of apo- and holo-flavodoxins to characterize qualitatively the polarity of the tryptophan environment and its accessibility for iodide. Then the time-resolved fluorescence and fluorescence anisotropy of *D. gigas* flavodoxin at a single emission wavelength are described using global analysis with 'arbitrary' multi-exponential functions leading to the best fit. A survey of decay parameters is then obtained. Fluorescence decays across the tryptophan emission band of apo- and holo-flavodoxins are analyzed to yield three-dimensional representations of time-resolved fluorescence, from which spectra at distinct times after the pulse are obtained. Theoretical rates of energy transfer between tryptophan and flavin are calculated from the 'known' *D. vulgaris* flavodoxin. Finally, a model is proposed to discuss the time-resolved fluorescence and fluorescence anisotropy: the data were re-analyzed globally to investigate the validity of the model.

Steady-state fluorescence

We have selectively excited the tryptophan residues of apo- and holo-flavodoxins at 295 nm. An example of absorption and emission spectra of *D. gigas* flavodoxin preparations is presented in Fig. 1. Fluorescence quenching experiments are given in Fig. 2 in the form of a Stern-Volmer and a modified Stern-Volmer plot. The results, relative quantum efficiencies, emission maxima and Stern-Volmer constants, are collected in Table 1. The most important features of Table 1 can be summarized as follows. From the emission maximum near 330 nm it can

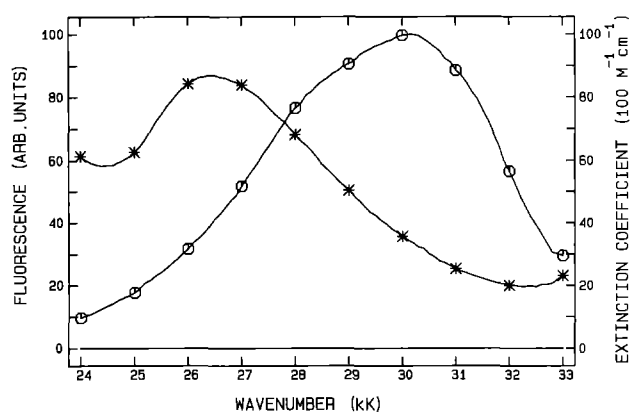


Fig. 1. Demonstration of the overlap between the emission spectrum of tryptophan (o) and the absorption spectrum of FMN (*) in *D. gigas* flavodoxin. The emission maximum of tryptophan in *D. gigas* FMN-depleted flavodoxin is located at 30.3 kK (330 nm). The molar extinction coefficient for FMN is $8700 \text{ M}^{-1} \text{ cm}^{-1}$ at 26.4 kK (379 nm)

Table 1. Steady-state fluorescence properties of *Desulfovibrio* flavodoxins at 20°C^a

| Sample | λ_{em}^b | q_r^c (nm) (± 0.02) | K_{sv}^d (M^{-1}) (± 0.02) |
|-------------------------|------------------|-----------------------------------|---|
| NATA | 358 | 1.00 | 10.40 |
| <i>D. gigas</i> apo | 330 | 0.73 | 0.30 |
| <i>D. gigas</i> holo | 330 | 0.19 | n.d. |
| <i>D. vulgaris</i> apo | 332 | 0.61 | 0.51 |
| <i>D. vulgaris</i> holo | 330 | 0.10 | n.d. |

^a Samples dissolved in 0.1 M Tris-HCl pH 7.5, apo is FMN-depleted flavodoxin, holo is native flavodoxin

^b Wavelength of maximum fluorescence

^c Relative quantum efficiency

^d Stern-Volmer constant

be concluded that the tryptophan residues are located in a rather apolar environment in both apo- and holo-proteins. The fact that there is hardly any change in emission maxima with or without FMN, indicates that to a first approximation the flavin does not perturb the electronic energy levels of the indole moiety. From the relative fluorescence efficiencies it is evident that FMN-binding results in a significant decrease of tryptophan fluorescence. This must be ascribed to radiationless excited-state energy transfer from tryptophan to flavin (Visser and Santema 1981). In Fig. 1 it is shown that there is a good overlap between the fluorescence spectrum of the single tryptophan (donor) and the absorption spectrum of the bound FMN (acceptor). The small initial slope in the Stern-Volmer plot (Fig. 2A) of the apo-flavodoxins should indicate that the tryptophan residues are accessible to the bulky iodide ion for low efficiency quenching. However, the ordinate intercept in the modified Stern-Volmer plot (Fig. 2B), reflecting the reciprocal fraction of accessible tryptophans indicates that a fraction of the tryptophan is totally inaccessible to quencher.

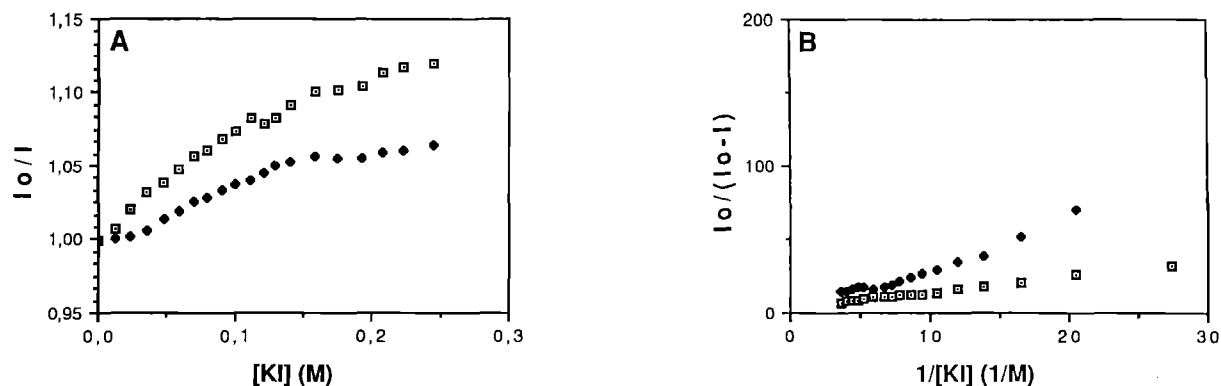


Fig. 2. Stern-Volmer plot (A) and modified Stern-Volmer plot (B) for quenching experiments of *D. gigas* and *D. vulgaris* FMN-depleted flavodoxin (see text for details). \blacklozenge : *D. gigas* flavodoxin, \square : *D. vulgaris* flavodoxin

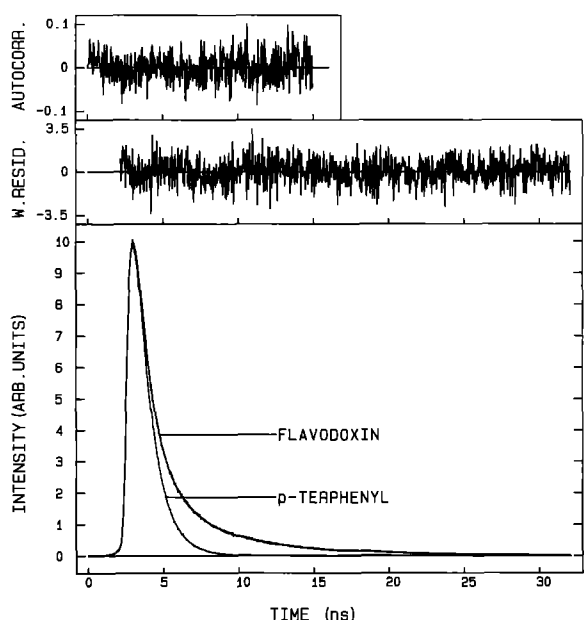


Fig. 3. Typical example of a fluorescence intensity decay analysis of *D. gigas* holo-flavodoxin in 0.1 M Tris-HCl pH 7.5 at 20°C. Excitation and emission wavelengths were 300 nm and 339 nm respectively. Both the fluorescence response of p-terphenyl in ethanol (τ_{ref} is 1.06 ns) and the experimental and calculated fluorescence decays (1000 channels, time equivalence 31 ps per channel) of *D. gigas* holo-flavodoxin are shown. The (three) fluorescence decay times, pre-exponential factors, and statistical parameters are collected in Table 2

Fluorescence decay and fluorescence anisotropy decay

In contrast to the exponential fluorescence decay of NATA (Vos et al. 1987), the fluorescence decay pattern of tryptophan in the flavodoxin is more complex. At least three exponentials are needed to fit the experimental decay. We have selected *D. gigas* apo- and holo-flavodoxin at 20°C to demonstrate the fit quality using a linear combination of exponential functions. An example of a best-fit decay analysis is shown in Fig. 3 for *D. gigas* holo-flavodoxin. Decay and statistical parameters for the various models have been collected in Table 2. The fluorescence decay of the holoprotein is distinctly more rapid

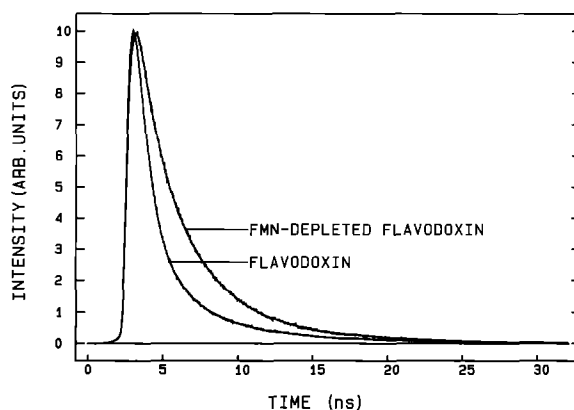


Fig. 4. Normalized fluorescence intensity decays of *D. gigas* FMN-depleted and holo-flavodoxin in 0.1 M Tris-HCl pH 7.5 at 20°C. Both experimental and calculated fluorescence intensity decays for both flavodoxin preparations are shown. Experimental conditions were identical to those described in the legend to Fig. 3. The fluorescence decay times, pre-exponential factors, and statistical parameters are listed in Table 2

than that of apo-flavodoxin. This is demonstrated in Fig. 4 where fluorescence decay profiles and their fits for *D. gigas* apo- and holoprotein are presented together. The more rapid fluorescence decay of the holoprotein arises from the much larger amplitude of the shortest lifetime component (cf. Table 2).

The fluorescence anisotropy decay of both *D. gigas* apo- and holo-flavodoxin was analyzed globally as well, using single- and double-exponential functions. For apo-flavodoxin a double exponential decay law does not improve the quality of the fit significantly (Fig. 5 A). For the holoprotein a double-exponential decay law was required to obtain a good fit to the data (see Fig. 5 B). Parameter values and statistical parameters are collected in Table 2. From the results in Table 2 it is clear that the anisotropy decay of holo-flavodoxin is characterized by a short and a long correlation time.

Time-resolved fluorescence spectra

We have also analyzed the fluorescence decay of the four protein preparations as a function of emission wave-

Table 2. Parameters describing the fluorescence decay (A) and fluorescence anisotropy decay (B) of *D. gigas* apo- and holo-flavodoxin at 20°C. Parameters (standard deviations are listed in parentheses) were calculated using a linear combination of exponential functions (λ_{exc} is 300 nm, λ_{em} is 339 nm, and band width is 5 nm)

| Sample | # ^a | α_1 | τ_1 (ns) | α_2 | τ_2 (ns) | α_3 | τ_3 (ns) | α_4 | τ_4 (ns) | χ_r^2 | DW ^b | ZP ^b |
|---|----------------|----------------|------------------|-----------------|------------------|----------------|------------------|-------------------------------|------------------------------|------------|-----------------|-----------------|
| A. Fluorescence decay | | | | | | | | | | | | |
| <i>D. gigas</i> apo | 1 | 1.00 (0.01) | 3.75 (0.01) | | | | | | | 27.3 | 0.06 | 2 |
| | 2 | 0.76 (0.01) | 2.40 (0.02) | 0.24 (0.01) | 6.00 (0.04) | | | | | 1.82 | 1.16 | 62 |
| | 3 | 0.18 (0.01) | 0.41 (0.04) | 0.67 (0.01) | 2.79 (0.03) | 0.15 (0.01) | 6.67 (0.08) | | | 1.13 | 1.81 | 199 |
| | 4 | 0.19 (0.01) | 0.38 (0.05) | 0.07 (0.14) | 2.21 (0.72) | 0.60 (0.13) | 2.85 (0.15) | 0.14 (0.02) | 6.70 (0.13) | 1.12 | 1.82 | 201 |
| <i>D. gigas</i> holo | 1 | 1.00 (0.01) | 2.56 (0.01) | | | | | | | 1.28 | 0.01 | 1 |
| | 2 | 0.93 (0.03) | 0.03 (0.01) | 0.07 (0.01) | 5.47 (0.02) | | | | | 1.88 | 0.84 | 8 |
| | 3 | 0.74 (0.01) | 0.89 (0.02) | 0.18 (0.01) | 2.80 (0.12) | 0.08 (0.01) | 6.74 (0.12) | | | 0.98 | 1.84 | 226 |
| | 4 | 0.61 (0.23) | 0.83 (0.07) | 0.16 (0.04) | 1.22 (0.38) | 0.16 (0.21) | 2.91 (0.52) | 0.07 (0.01) | 6.74 (0.21) | 0.99 | 1.87 | 231 |
| Sample | # ^d | β_1 | ϕ_1 (ns) | β_2 | ϕ_2 (ns) | χ_r^2 | DW ^b | ZP ^e | ZP _⊥ ^e | | | |
| B. Fluorescence anisotropy decay ^c | | | | | | | | | | | | |
| <i>D. gigas</i> apo | 1 | 0.22 (0.01) | 5.81 (0.08) | | | 1.12 | 1.84 | 201 | 205 | | | |
| | 2 | 0.26 (0.29) | 5.81 (2.10) | -0.04 (0.29) | 5.89 (14.30) | 1.12 | 1.84 | 203 | 205 | | | |
| <i>D. gigas</i> holo | 1 | 0.21 (0.01) | 4.74 (0.08) | | | 1.10 | 1.63 | 140 | 164 | | | |
| | 2 | 0.17 (0.02) | 2.69 (0.23) | 0.06 (0.02) | 22.15 (18.04) | 1.01 | 1.79 | 204 | 216 | | | |

^a Number of exponentials in the fluorescence decay function

^b DW is the Durbin-Watson parameter; ZP is the number of zero-passages of the autocorrelation function of the weighted residuals

^c Calculated using three exponentials describing the fluorescence decay

^d Number of exponentials in the fluorescence anisotropy decay function

^e ZP_{||} and ZP_⊥ are the number of zero-passages of the autocorrelation functions connected with parallel and perpendicular fluorescence intensity decays, respectively

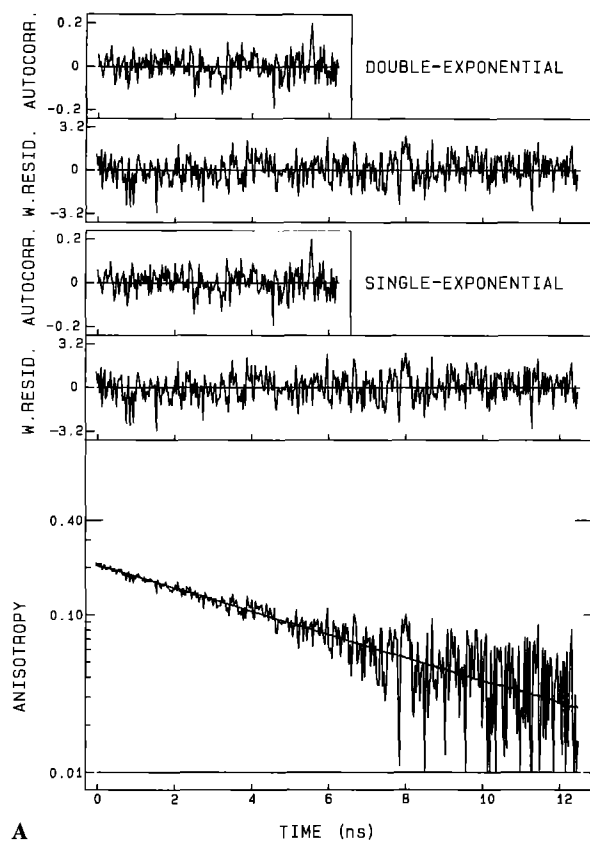
length. A three-dimensional representation of one data set is given in Fig. 6. From such a data set one can easily retrieve peak normalized spectra as a function of time. The average fluorescence lifetime increases at longer fluorescence wavelengths, implicating a spectral change during the decay. In Fig. 7 examples of fluorescence spectra at different times after a δ -pulse excitation are given for *D. gigas* apo- and holo-flavodoxin. It can be clearly seen that the fluorescence maximum shifts to the red from 330 nm to approximately 340 nm in the apoprotein. In the holoprotein it is evident that two maxima appear in the time-dependent emission. Similar changes were observed in *D. vulgaris* flavodoxin (Visser and Van Hoek 1988).

Energy transfer

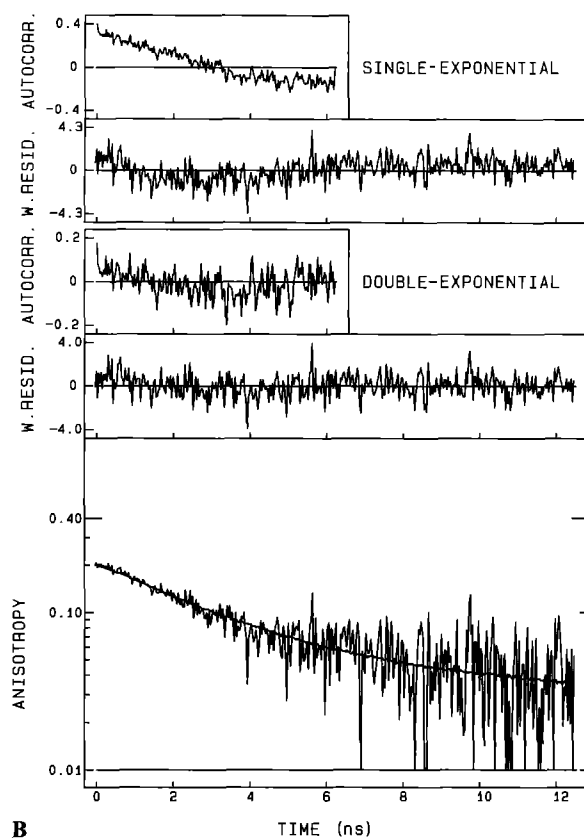
When the fluorescence decay characteristics of flavodoxin and FMN-depleted flavodoxin from both bacterial

sources are compared, it is clear that the relative weight of the shorter lifetime component is increased in the holo-protein (cf. Table 2). Energy transfer from tryptophan to flavin can explain the enhanced contribution of the short lifetime component. The photophysical behaviour of tryptophan, however, is complex. Two potentially fluorescent states (1L_a and 1L_b , ground state is denoted by 1A) are closely spaced in energy (Valeur and Weber 1977), with widely different polarization directions in the molecular frame (Yamamoto and Tanaka 1972) and with a high interconversion probability (Cross et al. 1983). The energy difference between the two states depends very much on the polarity of the direct environment of the indole moiety (Andrews and Forster 1974).

Since the 3-dimensional structure of the *D. vulgaris* flavodoxin is known (Watenpaugh et al. 1973), the transfer rate constants from each electronic level of both tryptophan residues to the single flavin acceptor can be evaluated, similarly to the assignments made for trypto-



A **Fig. 5A, B.** An example of fluorescence anisotropy decay analyses of *D. gigas* apo-flavodoxin (A) and holo-flavodoxin (B) in 0.1 M Tris-HCl pH 7.5 at 20°C. Both experimental and calculated fluorescence anisotropy decays are shown. The weighted residuals and the



B autocorrelation of the residuals of fitting with a single and a double exponential function are shown in the top panels. The fluorescence anisotropy decay parameters and statistical data are listed in Table 2

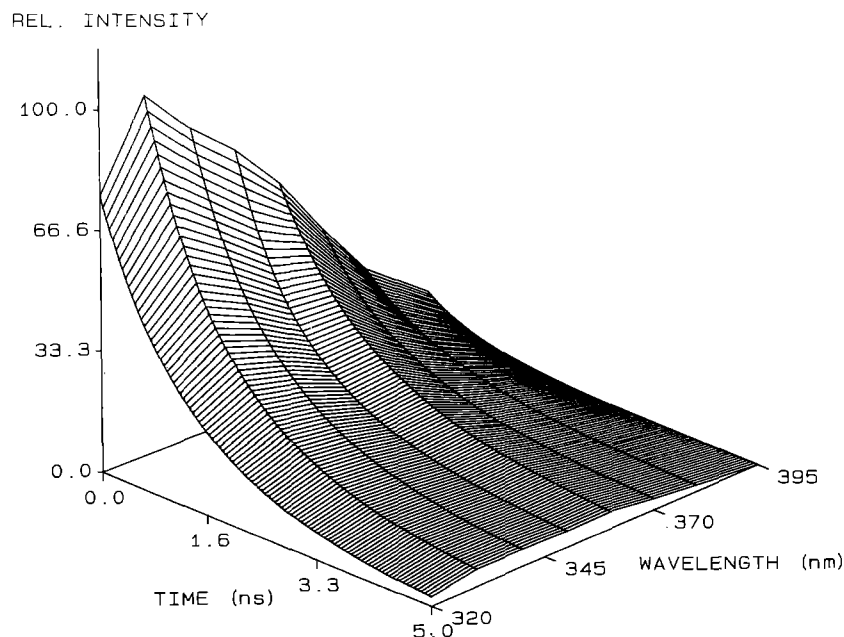


Fig. 6. Three-dimensional representation of a time-resolved fluorescence spectrum of *D. gigas* holo-flavodoxin constructed from a corrected steady-state fluorescence spectrum and deconvoluted fluorescence intensity decays for data collected at 320, 330, 340, 350, 360, 370, 380, and 395 nm

phan-heme transfer in myoglobin (Hochstrasser and Negus 1984). For simplicity we assumed in the calculations that the two excited states of the tryptophan can transfer independently and that both tryptophan residues exhibit Förster-type energy transfer. Also, the same over-

lap integral for the two tryptophan-flavin couples is assumed. The flavin accepts the energy via the second electronic state, its absorption vector in the molecular plane is known (Johansson et al. 1979). Since the relative orientations of transition dipoles as well as distances can be

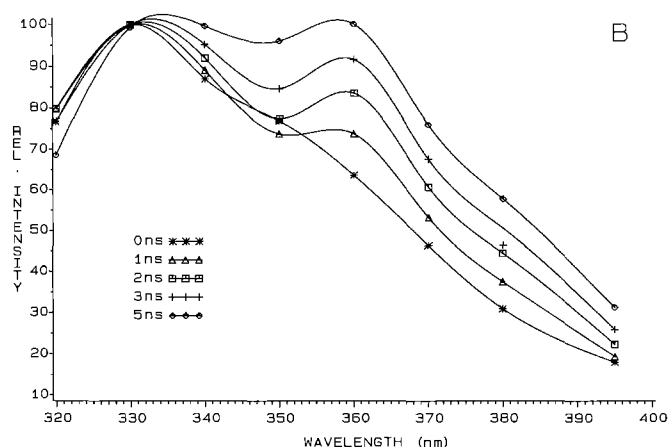
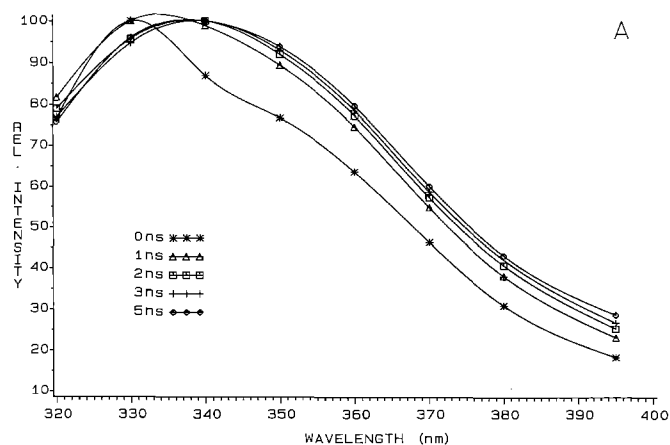


Fig. 7 A, B. Normalized fluorescence spectra of *D. gigas* FMN-depleted flavodoxin (A) and holo-flavodoxin (B). The curves are extracted from three-dimensional graphs (as in Fig. 6) by taking slices at times $t=0, 1, 2, 3$ and 5 ns. The fluorescence maximum shifts to

the red from 330 nm to approximately 340 nm in the FMN-depleted flavodoxin. In the holo-flavodoxin two maxima appear (second maximum at about 359 nm). The spectral changes were completed after approximately 5 ns

Table 3. Energy transfer rate constants (k_{DA}) calculated for *D. vulgaris* flavodoxin^a

| Donor | →Acceptor | R^b (Å) | κ^2^c | k_{DA}^d (s^{-1}) | τ_{DA} (ps) |
|------------------|-----------|--------------|--------------|----------------------------|---------------------|
| 1L_a (Trp60) | → FMN | 5.5 | 1.20 | $3.12 \cdot 10^{12}$ | 0.32 |
| 1L_b (Trp60) | → FMN | 5.5 | 0.06 | $1.56 \cdot 10^{11}$ | 6.4 |
| 1L_a (Trp140) | → FMN | 19.8 | 0.60 | $1.34 \cdot 10^9$ | 750 |
| 1L_b (Trp140) | → FMN | 19.8 | 0.17 | $1.90 \cdot 10^8$ | 5300 |

^a The constants were calculated from geometrical parameters using the 3-dimensional structure determined by Watenpaugh et al. (1973)

^b Center to center distance

^c κ^2 is the orientation factor

^d $k_{DA} = 1/\tau_{DA}$

determined, the transfer rate constants can be calculated (see Table 3). From inspection of Table 3 it is clear that the rate of transfer between the closest tryptophan (Trp 60) and FMN is at least two orders of magnitude larger than the transfer rate associated with the other tryptophan residue (Trp 140). The direct consequence is that fluorescence from this residue would be extinguished very rapidly. Another interesting result is the fact that transfer from the 1L_a electronic level is much more efficient than transfer from the 1L_b state for both tryptophans. This difference in transfer rate can be mainly ascribed to the less favourable orientation factor κ^2 (Dale et al. 1979). For the purpose of discussion the calculated rates can qualitatively explain the fluorescence decay patterns and the time-resolved wavelength shifts of flavodoxin. The increase in amplitude of the short lifetime component, when comparing apo- with holoprotein, can be accounted for by the finite energy transfer process. If the reciprocal transfer rate constants (τ_{DA} , see Table 3) connected with the 1L_a state are considered, it is evident that the time constant of transfer from Trp 140 (the remote one) is relatively long, of the same order as found

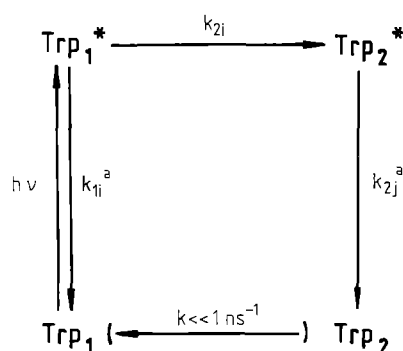


Fig. 8. Scheme describing an excited-state reaction of a tryptophan residue in a protein environment. The rate constant for this process is given by the symbol k_{2i} . Emission rate constants are indicated as well, with the superscript denoting either apoprotein (a) or holoprotein (h)

for the tryptophan-acceptor couple in lumazine protein (Kulinski et al. 1987).

Interpretation of fluorescence decay

The changes in emission spectra as a function of time observed for the single tryptophan in *D. gigas* flavodoxin indicate, in principle, two possibilities. The heterogeneity of the emission spectra arises either from at least two ground-state conformers with different excited-state behaviour or from the presence of an excited-state reaction on the nanosecond timescale. This reaction is not yet defined but it can originate from exciplex formation (Grinvald and Steinberg 1974), solvent relaxation (Gudgin-Templeton and Ware 1984) or in general, from relaxation into a different protein environment. A generalized scheme involving a uni-directional excited-state reaction and possibly consistent with the experimental data, for *D. gigas* at least, is given in Fig. 8. Trp_1^* in Fig. 8 is the primary excited species, Trp_2^* being populated from Trp_1^* . The kinetics associated with this scheme are similar

Table 4. Global lifetimes of the four different *Desulfovibrio* flavodoxin preparations, obtained by global analysis of fluorescence decay curves at different emission wavelengths

| Sample | | τ_1 (ns) | τ_2 (ns) | τ_3 (ns) | τ_4 (ns) | $\chi_r^2(4)^a$ | $\chi_r^2(3)^a$ |
|--------------------|------|------------------|------------------|------------------|------------------|-----------------|-----------------|
| <i>D. gigas</i> | apo | 0.13 | 1.23 | 3.67 | 9.10 | 1.63 | 2.25 |
| | holo | 0.12 | 1.11 | 3.84 | 10.0 | 1.33 | 2.63 |
| <i>D. vulgaris</i> | apo | 0.09 | 0.81 | 2.86 | 6.53 | 1.34 | 1.86 |
| | holo | 0.09 | 0.82 | 4.41 | 10.8 | 1.46 | 2.79 |

^a Global reduced $\chi_r^2(4)$ using a four-exponential decay function (with linked fluorescence lifetimes), $\chi_r^2(3)$ is the same but for a three-exponential decay function

to those derived for comparable cases, e.g. the interconversion of peptide conformers during the lifetime of the excited state (Donzel et al. 1974), exciplex formation (Grinvald and Steinberg 1974) or excited-state protonation (Laws and Brand 1979). The fluorescence decay is expected to be bi-exponential when both species are characterized by single fluorescence rate constants. The pre-exponential factors and lifetimes are functions of all the rate constants involved, while the solution of the system depends on the initial boundary conditions. When the fluorescence decays of the two species are multi-exponential the expressions take the following form:

$$I_1(t) \propto [\text{Trp}_1^*](t) = \sum_i \alpha_{1i}^a \exp[-k_{1i}^a \cdot t] \quad (7)$$

$$I_2(t) \propto [\text{Trp}_2^*](t) = \sum_i \sum_j \left\{ \frac{\alpha_{1i}^a \cdot \alpha_{2j}^a \cdot k_{2i}}{(k_{1i}^a - k_{2j}^a)} \right\} * (\exp[-k_{2j}^a \cdot t] - \exp[-k_{1i}^a \cdot t]) \quad (8)$$

with

$$\sum_i \alpha_{1i}^a = \sum_j \alpha_{2j}^a = 1.$$

In a first approximation we assume a general validity of the scheme for apo- and holoproteins (replace superscript a by h), i.e. any conformational change between apo- and holoprotein or resonance energy transfer in the holoprotein would not affect the scheme. When the microenvironments of the tryptophan residues in apo- and holoproteins are identical, the corresponding rate constants for the holoproteins are expected to be larger because of the additive involvement of the rate constant of energy transfer: $k^h = k^a + k_{\text{DA}}$. The two excited species, Trp_1^* and Trp_2^* , will have different spectral characteristics and the total fluorescence will be composed of two spectral contributions with wavelength-dependent weighting factors f_1 and $f_2 = \{1 - f_1\}$, for $[\text{Trp}_1^*]$ and $[\text{Trp}_2^*]$:

$$I(\lambda, t) = f_1(\lambda) I_1(t) + [1 - f_1(\lambda)] I_2(t) \quad (9)$$

$f_1(\lambda)$ being the fraction of emission at given wavelength λ associated with Trp_1^* such that:

$$f_1(\lambda) = \frac{F_1(\lambda)}{\int_0^\infty I_1(t) dt} = \frac{F_1(\lambda)}{\langle \tau \rangle} \quad (10)$$

where $F_1(\lambda)$ is the contribution of Trp_1^* fluorescence to the steady-state spectrum, $F(\lambda) = F_1(\lambda) + F_2(\lambda)$, and $\langle \tau \rangle$ is the

first-order average fluorescence lifetime of Trp_1^* . Global analytical approaches can be applied to resolve the two emission spectra from (9) since the rate constants of the decays at different emission wavelengths will be common. The next simplest case as compared to the bi-exponential decay model is for a mono-exponential fluorescence decay of Trp_1^* and a bi-exponential decay of Trp_2^* . Evaluation of (9) would result in a triple-exponential decay. A sum of three exponential functions, but with different pre-exponential factors, is also expected for the inverse case, namely a bi-exponential fluorescence decay of Trp_1^* and a single fluorescence rate constant for Trp_2^* . When both excited species are characterized by two fluorescence rate constants, the total fluorescence is expected to be composed of four exponential terms. The extension to a reversible excited-state reaction would result in more complicated rate equations and was not tried.

Although some parameters are also common between *D. gigas* apo- and holoproteins, global analysis across species was not carried out, because lifetimes of species taking part in energy transfer cannot be validly linked between apo- and holoprotein.

In the global analysis two model functions were tried: a linear combination of either three or four exponential terms in which all the lifetimes (or reciprocal rate constants) were linked between nine decay experiments at emission wavelengths between 320 and 405 nm. Based on the values for the global reduced χ_r^2 for both models the four-exponential model turned out to be the better model of the two since it resulted into a significantly lower χ_r^2 . The lifetimes and global reduced χ_r^2 values for both models have been listed in Table 4. As expected the relative amplitudes change with emission wavelength. The two shorter lifetime components (tentatively assigned to $[\text{Trp}_1^*]$) have a relatively larger weight than the two longer lifetime components (assigned to $[\text{Trp}_2^*]$). The amplitudes of the longer lifetime components, however, increase significantly at longer emission wavelength (at the cost of those of the shorter lifetimes). This is taken to indicate that the (predominant) contribution of Trp_1^* emission differs from that of the Trp_2^* emission. Using the results of global analysis we were able to resolve the steady-state fluorescence spectrum into two contributions arising from Trp_1^* and Trp_2^* . The results are given in Fig. 9. It can be noticed that the fluorescence of Trp_2^* is red-shifted as compared to that of Trp_1^* . This model is in complete agreement with the time-resolved spectral behaviour as presented in Fig. 7. The second species Trp_2^* has a much longer average lifetime so that its presence becomes apparent after the disappearance of Trp_1^* . The results summarized in Table 4 are also revealing with respect to energy transfer in the holoproteins. If attention is focussed on *D. gigas* flavodoxin only, the rate constants are of comparable magnitude. Only Trp_1^* would be involved in energy transfer since the lifetimes are shorter in the holoprotein. Rate constants of energy transfer of 0.6 ns^{-1} and 0.1 ns^{-1} are obtained from the two lifetime components of Trp_1^* in *D. gigas* apo- and holo-flavodoxin. It is worth noting that these rates are in the same order of magnitude as those calculated for energy transfer between Trp 140 and FMN in *D. vulgaris* flavodoxin. The lifetimes of Trp_2^*

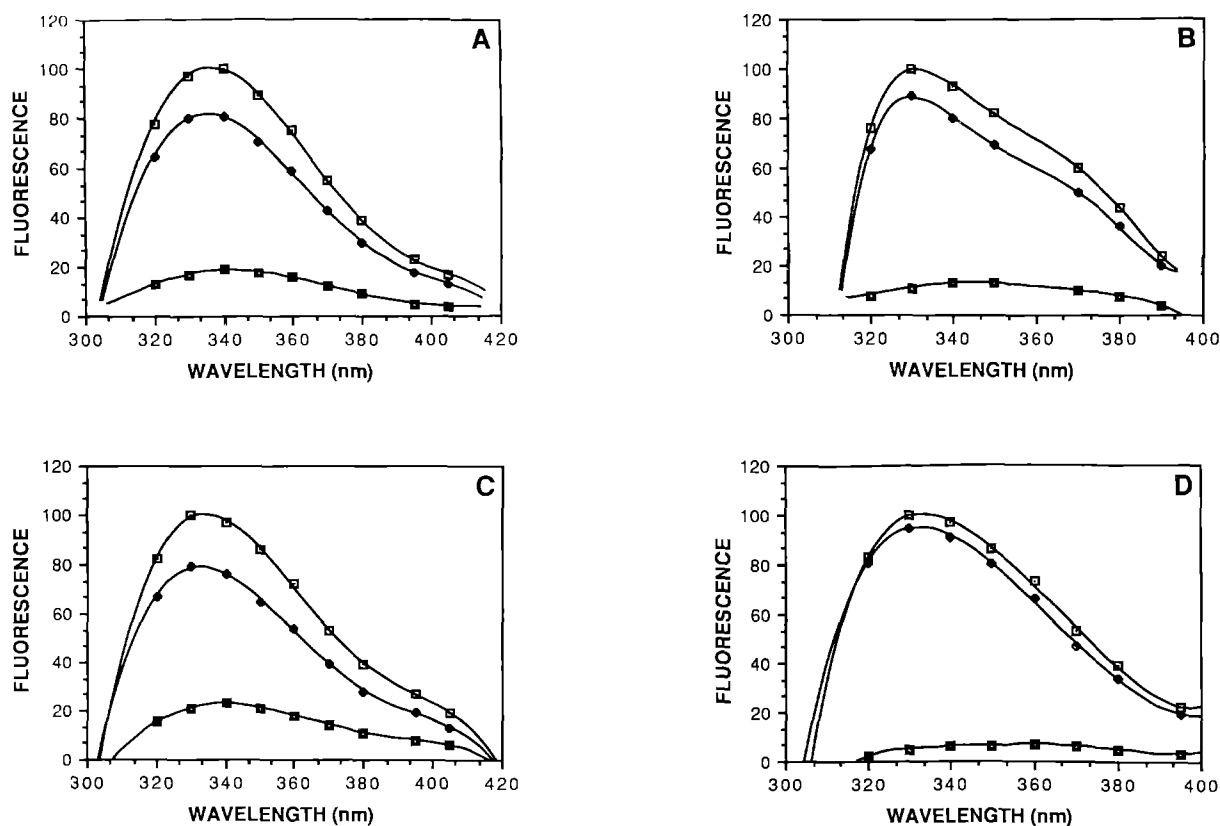


Fig. 9 A–D. Fluorescence spectra associated with Trp_1^* and Trp_2^* for four different *Desulfovibrio* flavodoxin preparations. A *D. gigas* apo-flavodoxin, B *D. gigas* holo-flavodoxin, C *D. vulgaris* apo-

flavodoxin, and D *D. vulgaris* holo-flavodoxin. $\square\square$: total fluorescence, $\circ\circ$: fluorescence of Trp_1^* , and $\blacksquare\blacksquare$: fluorescence of Trp_2^* . See Fig. 8 and text for details

are even slightly longer in the *D. gigas* holoprotein. The conclusion must therefore be that the microenvironment of the tryptophan is (slightly) altered upon binding of the flavin prosthetic group giving rise to somewhat different decay kinetics. Energy transfer is only manifested by quenching of the steady-state fluorescence spectrum of tryptophan and by an increase in amplitude of the short fluorescence lifetime component in the holoprotein (Table 2). Inspection of Table 4 reveals that there is no good correlation between the results from *D. vulgaris* apo- and holo-flavodoxins (the longer lifetime components are significantly longer in the holo-flavodoxin). However, there is some correlation between the lifetimes of *D. gigas* and *D. vulgaris* holo-flavodoxins. This result is interesting because it implies that the remote tryptophan residues in the two *Desulfovibrio* flavodoxins are very similar. The results of *D. vulgaris* apo-flavodoxin can be accounted for by the fact that both tryptophans are fluorescent now with different lifetimes and the lifetime values in Table 4 should be considered average values of emission from Trp 60 and Trp 140. The rate constants k_{21} and k_{22} for the conversion of Trp_1^* into Trp_2^* can be obtained, in principle, from the pre-exponential factors of the exponential functions. Evaluation of these amplitudes leads to a system of non-linear equations from which the rate constants can be obtained. We have estimated the rate constants for the case of *D. gigas* flavodoxin only at emission wavelengths between 320 and

370 nm. For apo-flavodoxin we found $k_{21} \cong 6 \pm 5 \text{ ns}^{-1}$ and $k_{22} = 0.52 \pm 0.20 \text{ ns}^{-1}$, and for the holo-flavodoxin $k_{21} \cong 2 \pm 1 \text{ ns}^{-1}$ and $k_{22} = 0.55 \pm 0.18 \text{ ns}^{-1}$. The rate constant k_{21} cannot be determined accurately because it can hardly be resolved, rate constant k_{22} on the other hand can be determined accurately and is identical for apo- and holo-flavodoxin. The reciprocal value of k_{22} indicates a relaxation time in the order of about 2 ns.

In the analysis of the fluorescence decay the assumption of two lifetime components for each species (two different microenvironments) is an over-simplification since the microenvironment of the tryptophan is probably more heterogeneous. For a more precise description a (multi-modal) distribution of fluorescence lifetimes should be taken into consideration (Alcala et al. 1987).

In principle, the expressions for the fluorescence decay (7) and (8) would also apply formally if Trp_1^* and Trp_2^* did actually correspond to 1L_a and 1L_b excited states produced. The 1L_a excited state is then directly produced from one ground state, while the 1L_b excited state is formed from the 1L_a excited state. The reversible case would be completely consistent with internal conversion between 1L_a and 1L_b states (Cross et al. 1983). Equilibrium of the two transitions is expected to occur very rapidly in the temperature range used (Andrews and Forster 1974; Ichiye and Karplus 1983). In this case the observed rate constants of fluorescence and of energy transfer will then be average values over the 1L_a and 1L_b transitions.

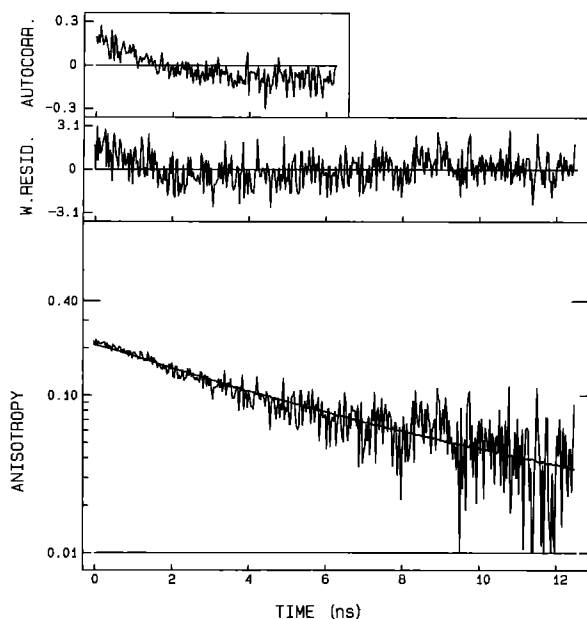


Fig. 10. Results of fitting of experimental fluorescence anisotropy decay data of *D. gigas* holo-flavodoxin (4 °C) with the model given in (14). Parameters and global reduced χ_r^2 are given in Table 5

Interpretation of fluorescence anisotropy decay

The rotational correlation times of the apo-flavodoxins (20 °C) obtained after single exponential analysis are in good agreement with the molecular weight of the proteins ($M_r = 15$ kDa) using the empirical formula (Visser et al. 1983 b):

$$\phi = 3.84 * 10^{-4} M_r \quad (11)$$

with ϕ in ns and M_r in Da. The calculated correlation time is 5.8 ns. An important conclusion that can be drawn from the results presented in Table 2 is that the tryptophan residues in the apo-flavodoxins are immobilized on the nanosecond time-scale, thus they are rotating with the whole protein. On the other hand, the two holo-flavodoxins exhibit anomalous anisotropy decay with a short and a long correlation time. When the fluorescence anisotropy decay data of the holo-flavodoxins (at different temperatures) are analyzed using a bi-exponential decay model (single-exponential analysis did not result in good fits), it is found that the short correlation time is in the range of 1–3 ns and the long correlation time is in the range of 15–30 ns. In a first approximation the long correlation time would indicate a large particle with molecular weight of 40–80 kDa. However, the protein preparation was shown to be homogeneous by a variety of analytical biochemical methods and no aggregation was found under the conditions used. Also, extreme elongation which can account for heterogeneous anisotropy decay can be ruled out since the protein shape is nearly spherical (Watenpaugh et al. 1973). This led us to seek another explanation, which fits nicely with the concepts developed in the previous section.

Considering the proposed model to explain the fluorescence decay data (Fig. 8), the fluorescence anisotropy

decay will also be dependent on the emission wavelength:

$$r(\lambda, t) = \left\{ \frac{f_1(\lambda) \cdot I_1(t) \cdot r_1(0) + \{1 - f_1(\lambda)\} \cdot I_2(t) \cdot r_2(0)}{f_1(\lambda) \cdot I_1(t) + \{1 - f_1(\lambda)\} \cdot I_2(t)} \right\} * \exp[-t/\phi] \quad (12)$$

where ϕ is the rotational correlation time of the protein. This expression predicts non-exponential anisotropy decay for all wavelengths at which the two emission spectra overlap.

We have globally analyzed the polarized fluorescence decay curves of both apo- and holo-flavodoxins at different temperatures and at a single emission wavelength in order to recover an optimum correlation time ϕ and a value for $r(0)$ (we have ignored the 0.1 ns longer time arising from the contribution of FMN). We have tried to fit the anisotropy decay data according to (12) for sets of apo- and holo-flavodoxins. As judged from the fitting criteria, however, the results were not satisfactory. The globally obtained correlation times were distinctly shorter than the ones obtained from separate analysis of the anisotropy decay of apo-flavodoxin. These results suggest that (12) is not adequate and that an extra depolarization process must be operative in the two holo-flavodoxins. This process is probably related to the type of energy transfer as described in the previous section. Therefore the data were re-analyzed using the model as described in (12) for apo-flavodoxin and an empiric decay function which described the anomalous decay in the holo-flavodoxin:

$$r^a(t) = \beta_1^a \cdot \exp[-t/\phi] \quad (13)$$

$$r^h(t) \approx (\beta_1^h + \beta_2^h \cdot \exp[-t/\phi_s]) \cdot \exp[-t/\phi] \quad (14)$$

where

$$\beta_1^h + \beta_2^h \approx \beta_1^a.$$

Here, (13) is, in principle, identical to (12) and (14) contains an extra exponential term accounting for an additional depolarization with correlation time ϕ_s ; superscripts *a* and *h* refer to apo- and holo-flavodoxin, respectively. The nature of this depolarization is not known, but it may arise from segmental motion or energy transfer. This decay model, though not exact, gave much better fits to the data. A typical example of the analysis of *D. gigas* holo-flavodoxin is given in Fig. 10. If the additional depolarization is due to energy transfer, the correlation time ϕ_s contains information on the rate of energy transfer: $\phi_s^{-1} = k_{DA} + \phi^{-1}$. All anisotropy parameters including the rate constant of energy transfer are collected in Table 5. It should be stressed that the model described by (14) is not exact. The relaxation of the tryptophan residue into another microenvironment, already present in the apo-flavodoxin, is a complicating factor because it apparently takes place on the same time scale as the energy transfer process. Nonetheless, the analyzed anisotropy results yield a realistic rotational correlation time for apo- and holo-flavodoxins. Furthermore, the anisotropy analysis yields, for *D. vulgaris* flavodoxin, a rate constant of energy transfer of the same order of magnitude as the one determined from the crystal structure (cf. Table 3). In addition, for *D. gigas* flavodoxin, the rate constant of energy trans-

Table 5. Global correlation times and other anisotropy parameters of the four different *Desulfovibrio* flavodoxin preparations at various temperatures according to (13) and (14). The rotational correlation time ϕ of the apoprotein, as calculated in single exponential decay analysis, has been linked with the correlation time ϕ of the holoprotein. The correlation times ϕ were fixed at the values of the apoprotein, which gave better fits

| Sample | T (°C) | β_1 (± 0.01) | ϕ (ns) (-) | β_2 (± 0.02) | ϕ_s (ns) (± 0.3) | k_{DA} (ns^{-1}) | $r(0)$ (± 0.03) | χ_r^2 ^a |
|--------------------|-------------|-----------------------------|-----------------------|-----------------------------|-----------------------------------|----------------------------------|--------------------------|-------------------------|
| <i>D. gigas</i> | apo | 4 | 0.22 | 8.3 | | | 0.22 | 1.21 |
| | holo | 4 | 0.15 | 8.3 | 0.08 | 2.8 | 0.2 | 0.23 |
| | apo | 20 | 0.22 | 5.8 | | | | 0.22 |
| | holo | 20 | 0.18 | 5.8 | 0.04 | 1.3 | 0.6 | 0.22 |
| | apo | 30 | 0.22 | 4.5 | | | | 0.22 |
| | holo | 30 | 0.16 | 4.5 | 0.05 | 1.6 | 0.4 | 0.21 |
| <i>D. vulgaris</i> | apo | 4 | 0.24 | 9.2 | | | 0.24 | 1.32 |
| | holo | 4 | 0.21 | 9.2 | 0.02 | 0.4 | 2.5 | 0.23 |
| | apo | 20 | 0.24 | 5.3 | | | | 0.24 |
| | holo | 20 | 0.23 | 5.3 | 0.01 | 0.5 | 1.7 | 0.24 |
| | apo | 30 | 0.23 | 4.1 | | | | 0.23 |
| | holo | 30 | 0.22 | 4.1 | 0.02 | 0.6 | 1.4 | 0.24 |

^a Global reduced χ_r^2 , obtained after globally analyzing the decay curves of apo- and holo-flavodoxins at a particular temperature

fer turns out to be comparable to the ones obtained from time-resolved fluorescence decay analysis (0.6 ns^{-1} and 0.1 ns^{-1}).

Conclusion

The fluorescence decay kinetics of tryptophan can be modeled according to a scheme describing a relaxation process, in which the interaction of the tryptophan residue with its environment changes on the nanosecond time range. Such an excited-state reaction takes place in both apo- and holo-flavodoxin. Preferential energy transfer from the originally excited state of tryptophan to the flavin acceptor appears to be a realistic mechanism. *D. gigas* flavodoxin contains a single tryptophan residue. The amino acid sequence of this protein is unknown. An important conclusion can be drawn from the fluorescence decay data. If the tryptophan is located close to FMN, there would be extremely efficient energy transfer (cf. Table 3) and the fluorescence would be extinguished very rapidly. Since this is not the case and because of the close resemblance of decay patterns and (time-resolved) fluorescence spectra between both flavodoxins, it is likely that the remote tryptophan residue is preserved in both flavodoxins. The center of this tryptophan must then be located at about 20 Å from the center of the isoalloxazine ring-system. *D. vulgaris* flavodoxin with its two tryptophan residues is too complex a system for quantification of its fluorescence in apo- and holo-flavodoxin. On the other hand, the gene encoding the *D. vulgaris* flavodoxin has been cloned and expressed in *Escherichia coli* (Krey et al. 1988), so this flavodoxin lends itself for site-directed mutagenesis, in which either one of the tryptophans can be replaced by other non-fluorescent amino acids leading in this way to a complete understanding of the protein fluorescence.

A final concluding remark should be made on the comparison of tryptophan fluorescence in apo- and holo-

flavodoxin. Removal of FMN results into an altered microenvironment of the tryptophan residue(s) which shows up as different fluorescence kinetics of the two protein preparations. This impedes a straightforward determination of, for instance, the rate constant of energy transfer between tryptophan and flavin.

Acknowledgements. We wish to acknowledge Prof. J. M. Beechem and Prof. L. Brand for kindly making available the global analysis programs. We thank Mrs. J. C. Toppenberg-Fang and Ms. E. Verberne for assistance in the preparation of the manuscript. Financial support was obtained from The Netherlands Organization for Scientific Research (N.W.O.) and from NSF grant DMB-8602789 (to J. LeGall).

References

- Alcala JR, Gratton E, Prendergast FG (1987) Fluorescence lifetime distributions in proteins. *Biophys J* 51:597–604
- Andrews LJ, Forster LS (1974) Fluorescence characteristics of indoles in non-polar solvents: lifetimes, quantum yields and polarization spectra. *Photochem Photobiol* 19:353–360
- Beechem JM, Brand L (1985) Time-resolved fluorescence of proteins. *Ann Rev Biochem* 54:43–71
- Beechem JM, Ameloot M, Brand L (1985a) Global analysis of fluorescence decay surfaces: excited-state reactions. *Chem Phys Lett* 120:466–472
- Beechem JM, Ameloot M, Brand L (1985b) Global and target analysis of complex decay phenomena. *Anal Instrum* 14:379–402
- Brand L, Knutson JR, Davenport L, Beechem JM, Dale RE, Walbridge DG, Kowalczyk AA (1985) Time-resolved fluorescence spectroscopy: some applications of associative behaviour to studies of proteins and membranes. In: Bayley PM, Dale RE (eds) *Spectroscopy and the dynamics of molecular biological systems*. Academic Press, London, pp 259–309
- Burnett RM, Darling GD, Kendall DS, LeQuesne ME, Mayhew SG, Smith WW, Ludwig ML (1974) Structure of the oxidized form of *Clostridial* flavodoxin at 1.9 Å resolution. Description of the flavin mononucleotide binding site. *J Biol Chem* 249:4383–4392
- Chang MC, Petrich JW, McDonald DB, Fleming GR (1983) Nonexponential fluorescence decay of tryptophan, tryptophylglycine, and glycyltryptophan. *J Am Chem Soc* 105:3819–3824

- Creed D (1984) The photophysics and photochemistry of the near-UV absorbing amino acids. I. Tryptophan and its simple derivatives. *Photochem Photobiol* 39:537–562
- Cross AJ, Waldeck DH, Fleming GR (1983) Time resolved polarization spectroscopy: level kinetics and rotational diffusion. *J Chem Phys* 78:6455–6467
- Cundall RB, Dale RE (eds) (1983) Time-resolved fluorescence spectroscopy in biochemistry and biology. NATO ASI Series, Ser A: Life sciences, vol 69. Plenum Press, New York London
- Dale RE, Eisinger J, Blumberg WE (1979) The orientational freedom of molecular probes; the orientation factor in intramolecular energy transfer. *Biophys J* 26:161–194
- D'Anna JA, Tollin G (1972) Studies of flavin-bound interaction in flavoproteins using protein fluorescence and circular dichroism. *Biochemistry* 11:1073–1080
- Donzel B, Gauduchon P, Wahl Ph (1974) Study of the conformation in the excited state of two tryptophanyl diketopiperazines. *J Am Chem Soc* 96:801–808
- Dubourdieu M, LeGall J (1970) Chemical study of two flavodoxins extracted from sulfate reducing bacteria. *Biochem Biophys Res Commun* 38:965–972
- Easter JH, DeToma RP, Brand L (1976) Nanosecond time-resolved emission spectroscopy of a fluorescence probe adsorbed to *L*- α -egg lecithin vesicles. *Biophys J* 16:571–583
- Eaton WA, Hofrichter J, Makinen MW, Andersen RD, Ludwig ML (1975) Optical spectra and electronic structure of flavine mononucleotide in flavodoxin crystals. *Biochemistry* 14:2146–2151
- Edmondson DE, Tollin G (1971) Chemical and physical characterization of the Shethna flavoprotein and apoprotein and kinetics and thermodynamics of flavin analog binding to the apoprotein. *Biochemistry* 10:124–133
- Eisinger J, Feuer B, Lamola AA (1969) Intramolecular singlet excitation transfer. Applications to polypeptides. *Biochemistry* 8:3908–3914
- Förster T (1965) Delocalized excitation and excitation transfer. In: Sinanoglu O (ed) *Modern quantum chemistry, part III*. Istanbul international school of quantum chemistry lectures. Academic Press, New York, pp 93–137
- Fox JL, Heumann H (1982) Flavin mononucleotide binding by *Desulfovibrio gigas* flavodoxin. In: Massey V, Williams CH (eds) *Flavins and flavoproteins*. Elsevier, Amsterdam, pp 500–503
- Grinvald A, Steinberg IZ (1974) Fast relaxation processes in a protein revealed by the decay kinetics of tryptophan fluorescence. *Biochemistry* 13:5170–5178
- Gudgin-Templeton EF, Ware WR (1984) The time dependence of the low-temperature fluorescence of tryptophan. *J Phys Chem* 88:4626–4631
- Hochstrasser RM, Negus DK (1984) Picosecond fluorescence decay of tryptophans in myoglobin. *Proc Natl Acad Sci USA* 81:4399–4403
- Ichiye T, Karplus M (1983) Fluorescence depolarization of tryptophan residues in proteins: a molecular dynamics study. *Biochemistry* 22:2884–2893
- Irwin RM, Visser AJWG, Lee J, Carreira LA (1980) Protein-ligand interactions in lumazine protein and in *Desulfovibrio* flavodoxins from resonance coherent anti-Stokes Raman spectra. *Biochemistry* 19:4639–4646
- Johansson LB-Å, Davidsson Å, Lindblom G, Razi Naqvi K (1979) Electronic transitions in the isoalloxazine ring and orientation of flavins in model membranes studied by polarized light spectroscopy. *Biochemistry* 18:4249–4253
- Knutson JR, Beechem JM, Brand L (1983) Simultaneous analysis of multiple fluorescence decay curves: a global approach. *Chem Phys Lett* 102:501–507
- Krey GD, Vanin EF, Swenson RP (1988) Cloning, nucleotide sequence, and expression of the flavodoxin gene from *Desulfovibrio vulgaris* (Hildenborough). *J Biol Chem* 263:15436–15443
- Kulinski T, Visser AJWG, O'Kane DJ, Lee J (1987) Spectroscopic investigations of the single tryptophan residue and of riboflavin and 7-oxolumazine bound to lumazine apoprotein from *Photobacterium leiognathi*. *Biochemistry* 26:540–549
- Lakowicz JR (1983) *Principles of fluorescence spectroscopy*. Plenum Press, New York
- Laws WR, Brand L (1979) Analysis of two-state excited state reactions. The fluorescence decay of 2-naphthol. *J Phys Chem* 83:795–802
- LeGall J, Forget N (1978) Purification of electron-transfer components from sulphate-reducing bacteria. *Methods Enzymol* 53:613–634
- LeGall J, Hatchikian ET (1967) Purification et propriétés d'une flavoprotéine intervenant dans la réduction du sulphite par *Desulfovibrio gigas*. *C R Acad Sci Paris* 264:2580–2583
- Lehrer SS (1971) Solute perturbation of protein fluorescence. The quenching of the tryptophyl fluorescence of model compounds and of lysozyme by iodide ion. *Biochemistry* 10:3254–3263
- Longworth JW (1983) Intrinsic fluorescence in proteins. In: Cundall RB, Dale RE (eds) *Time-resolved fluorescence spectroscopy in biochemistry and biology*. Plenum Press, New York, pp 651–725
- Mayhew SG, Ludwig ML (1975) Flavodoxins and electron-transferring flavoproteins. In: Boyer PD (ed) *The enzymes*. Academic Press, New York, pp 57–118
- Munro I, Pecht I, Stryer L (1979) Subnanosecond motions of tryptophan residues in proteins. *Proc Natl Acad Sci USA* 76:56–60
- Petrich JW, Chang MC, McDonald DB, Fleming GR (1983) On the origin of nonexponential fluorescence decay in tryptophan and its derivatives. *J Am Chem Soc* 105:3824–3832
- Rigler R, Ehrenberg M (1973) Molecular interactions and structure as analyzed by fluorescence relaxation spectroscopy. *Q Rev Biophys* 6:139–199
- Rigler R, Ehrenberg M (1976) Fluorescence relaxation spectroscopy in the analysis of macromolecular structure and motion. *Q Rev Biophys* 9:1–19
- Ryan J, Tollin G (1973) Flavine-protein interactions in flavoenzymes. Effect of chemical modification of tryptophan residues upon flavine mononucleotide binding and protein fluorescence in *Azotobacter* flavodoxin. *Biochemistry* 12:4550–4554
- Simondson RP, Tollin G (1980) Structure-function relations in flavodoxins. *Mol Cell Biochem* 33:13–24
- Smith WW, Patridge KA, Ludwig ML, Petsko GA, Tsernoglou D, Tanaka M, Yasunobu KT (1983) Structure of oxidized flavodoxin from *Anacystis nidulans*. *J Mol Biol* 165:737–755
- Szabo AG, Rayner DM (1980) Fluorescence decay of tryptophan conformers in aqueous solution. *J Am Chem Soc* 102:554–563
- Tollin G, Edmondson DE (1980) Purification and properties of flavodoxins. *Methods Enzymol* 69:392–406
- Valeur B, Weber G (1977) Resolution of the fluorescence excitation spectrum of indole into the 1L_a and 1L_b excitation bands. *Photochem Photobiol* 25:441–444
- Van Hoek A, Vervoort J, Visser AJWG (1983) A subnanosecond resolving spectrofluorimeter for the analysis of protein fluorescence kinetics. *J Biochem Biophys Methods* 7:243–254
- Van Hoek A, Visser AJWG (1985) Artefact and distortion sources in time-correlated single photon counting. *Anal Instrum* 14:359–378
- Van Hoek A, Vos K, Visser AJWG (1987) Ultrasensitive time-resolved polarized fluorescence spectroscopy as a tool in biology and medicine. *IEEE J Quantum Electron* QE-23:1812–1820
- Vervoort J, Müller F, LeGall J, Bacher A, Sedlmaier H (1985) Carbon-13 and nitrogen-15 nuclear magnetic resonance investigation on *Desulfovibrio vulgaris* flavodoxin. *Eur J Biochem* 151:49–57
- Vervoort J, Müller F, Mayhew SG, Van den Berg WAM, Moonen CTW, Bacher A (1986) A comparative carbon-13, nitrogen-15, and phosphorus-31 nuclear magnetic resonance study on the flavodoxins from *Clostridium MP*, *Megasphaera elsdenii*, and *Azotobacter vinelandii*. *Biochemistry* 25:6789–6799
- Visser AJWG, Santema JS (1981) Preferred conformation of flavinyl tryptophan peptides revealed by polarized excitation energy transfer. *Photobiochem Photobiophys* 3:125–133
- Visser AJWG, Van Hoek A (1988) The application of picosecond-resolved fluorescence spectroscopy in the study of flavins and

- flavoproteins. In: Lakowicz JR (ed) Time-resolved laser spectroscopy in biochemistry. Proceedings of SPIE – The International Society for Optical Engineering, vol 909, pp 61–68
- Visser AJWG, Li TM, Drickamer HG, Weber G (1977) Effect of pressure upon the fluorescence of various flavodoxins. *Biochemistry* 16:4879–4882
- Visser AJWG, Carreira LA, LeGall J, Lee J (1980) Coherent anti-Stokes Raman spectroscopy of flavodoxin in solution and crystal phases. *J Phys Chem* 84:3344–3346
- Visser AJWG, Vervoort J, O’Kane DJ, Lee J, Carreira LA (1983 a) Raman spectra of flavin bound in flavodoxins and in other flavoproteins. Evidence for structural variations in the flavin binding region. *Eur J Biochem* 131:639–645
- Visser AJWG, Penners NHG, Müller F (1983 b) Dynamic aspects of protein-protein association revealed by anisotropy decay measurements. In: Sund H, Veeger C (eds) *Mobility and recognition in cell biology*. de Gruyter, Berlin New York, pp 137–152
- Visser AJWG, Ykema T, Van Hoek A, O’Kane DJ, Lee J (1985) Determination of rotational correlation times from deconvoluted fluorescence anisotropy decay curves. Demonstration with 6,7-dimethyl-8-ribityllumazine and lumazine protein from *Photobacterium leiognathi* as fluorescent indicators. *Biochemistry* 24:1489–1496
- Visser AJWG, Van Hoek A, Kulinski T, LeGall J (1987) Time-resolved fluorescence studies of flavodoxin. Demonstration of picosecond fluorescence lifetimes of FMN in *Desulfovibrio* flavodoxins. *FEBS Lett* 224:406–410
- Vos K, Van Hoek A, Visser AJWG (1987) Application of a reference convolution method to tryptophan fluorescence in proteins. A refined description of rotational dynamics. *Eur J Biochem* 165:55–63
- Wassink JH, Mayhew SG (1975) Fluorescence titration with apoflavodoxin: a sensitive assay for riboflavin 5'-phosphate and flavin adenine dinucleotide in mixtures. *Anal Biochem* 68:609–616
- Watenpaugh KD, Sieker LC, Jensen LH (1973) The binding of riboflavin-5'-phosphate in a flavoprotein: flavodoxin at 2.0 Å resolution. *Proc Natl Acad Sci USA* 70:3857–3860
- Yamamoto Y, Tanaka J (1972) Polarized absorption spectra of crystals of indole and its related compounds. *Bull Chem Soc Jpn* 45:1362–1366